Short communication

Preparation of Trimetallic Composite Nanoparticles $Pd_xNi_yFe_z$ by a Pyrolysis Method in the Solvent of Ionic Liquids for Ethanol Oxidation Reaction

Keqiang Ding[*]*, Yongbo Zhao, Lu Liu, Yuan Li, Jing Zhao, Yuying Chen, Jiamiao Niu, Qingfei Wang*[*]

College of Chemistry and Materials Science, Hebei Normal University, Shijiazhuang 050024, P.R. China
[*]E-mail: dkeqiang@263.net; wqfxt@126.com

Trimetallic composite nanoparticles of $Pd_xNi_yFe_z$ (the nominal atomic ratios of Pd : Ni: Fe are 1:1:1,1:1.5:1,1:1:1.5,1:1:3 and 1:0:3, respectively) supported on multi-walled carbon nanotubes (MWCNTs) (denoted as $Pd_xNi_yFe_z$/MWCNTs) have been prepared by a pyrolysis method using room temperature ionic liquids (RTILs) of 1-n-Butyl-3-methylimidazolium triflate ([BMIM]OTF) as the solvent. The structure and morphology of the samples were thoroughly characterized using X-ray diffraction (XRD), scanning electron microscope (SEM) and transmission electron microscopy (TEM). Ethanol oxidation reaction (EOR) was investigated on the as-prepared catalysts by employing cyclic voltammetry (CV), demonstrating that the largest peak current of EOR was exhibited on the $Pd_1Ni_1Fe_{1.5}$/MWCNTs coated glassy carbon electrode. The smaller particle size and relatively lower open circuit electrode potential were thought as the main reasons for the excellent electrocatalysis of the $Pd_1Ni_1Fe_{1.5}$/MWCNTs toward EOR when compared to other catalysts.

1. INTRODUCTION

Owing to the high efficiency and low pollution levels, direct alcohol fuel cells (DAFCs) have received increasing attention as power sources for electronic devices and portable vehicles. Among those developed types of DAFCs, ethanol fuel cells (DEFCs) are promising power sources thanks to its high energy density, low pollutant emission, low operating temperature, and easy handling [1]. More importantly, ethanol, the fuel of DEFCs, is a green and renewable resource that can be facilely

produced from agricultural products [2]. It is well known that platinum (Pt) and Pt-based electrocatalysts are the most effective catalysts for the electrooxidation of ethanol in DEFCs [3]. However, recent works have revealed that when using Pt and Pt-based electrocatalysts, the kinetics of EOR remains sluggish and the complete electro-oxidation of ethanol is difficult to achieve, thus, leading to a low efficiency of ethanol oxidation which greatly limits the further development of DEFCs [4]. Fortunately, recently published works have showed that Palladium (Pd) is a good electro-catalyst for ethanol oxidation in alkaline media, and therefore, Pd is considered to be a promising candidate for Pt mainly due to the following reasons (ⅰ) Pd possesses similar electronic structure as Pt; (ⅱ) Pd is considerably less expensive than Pt; (ⅲ) Pd is much more abundant on the earth when compared to Pt [5]. As a result, great efforts have been devoted to prepare various Pd and Pd-based materials or nanomaterials with an intention to further lower its producing cost while enhancing its catalytic activity.

Employing ternary metallic nanoparticles as the catalysts for an electrochemical reaction was regarded as an effective way to improve the electrocatalytic activity of a pure noble metal catalyst while lowering its cost. For example, catalysts of PtCuAg [6] and Pt-Pd-Cu [7] were developed for oxygen reduction reaction (ORR), and Pt-Ni-Cr [8], Pt-Sn-Ce [9], PtSnIn [10], and Pt-Sn-Pr [11] were prepared for methanol oxidation reaction (MOR) or ethanol oxidation reaction (EOR). Although numerous papers concerning the preparation and property of Pd-based bimetallic nanoparticles as electrocatalysts for EOR have been published [12], the works relating to the Pd-based trimetallic nanocatalysts for EOR are rarely reported. Datta et al. synthesized [13] vulcan XC-72 supported ternary catalysts of PtPdAu/C under borohydride reduction scheme and studied their electrocatalytic activity toward EOR in alkaline media at room temperature. He pointed out that Au and Pd incorporation into the Pt matrix not only increased the catalytic efficiency of the alloyed catalysts but also effectively reduced the Pt content in the ternary system. Cai et al. [14] researched EOR on dealloyed Pd-Ni-P film in alkaline media, in which Pd-Ni-P film was prepared via electro-deposition on Au substrate. He thought that the enhanced electrocatalysis was attributed to the formation of both CO_{ad} and acetate. To the best of our knowledge, no paper reporting the preparation of Pd-Ni-Fe ternary nanoparticles was published so far.

As a novel media, room temperature ionic liquids (RTILs) have attracted great attention largely due to their excellent properties including low-volatility, non-toxicity and higher conductivity compared to common organic solvents, and higher solubility for organic substances compared with aqueous solutions. However, besides the high price, the inherent property of them such as the higher viscosity has greatly restricted their further applications. Therefore, developing novel application is very pivotal for the finial commercialization of RTILs. In summary, being utilized as solvent in organic synthesis [15] and electrolyte [16] in electrochemistry are the key applications of RTILs. To our knowledge, except our previous work [17], reports on the application of RTILs in a pyrolysis process are rare.

In this paper, five kinds of $Pd_xNi_yFe_z$/MWCNT nanocomposite catalysts having various atomic ratios were prepared by a one-pot method of pyrolysis, where RTILs of 1-n-Butyl-3-methylimidazolium triflate ([BMIM]OTF) was utilized as the solvent. Scanning electron microscopy (SEM), transmission electron microscopy (TEM) and x-ray diffraction (XRD) were thoroughly

employed to characterize the morphology and crystalline structures of the as-synthesized $Pd_xNi_yFe_z$/MWCNTs. Cyclic voltammetry (CV) and chronoamperometry were utilized to study the electrochemical activities of the as-prepared catalysts for EOR. Possible reasons for the superior electrocatalytic activity of the $Pd_1Ni_1Fe_{1.5}$ /MWCNTs towards EOR were also discussed.

2. EXPERIMENT

2.1 Materials

Room temperature ionic liquid of 1-n-Butyl-3-methylimidazolium triflate ([BMIM]OTF) with a purity of more than 99% was obtained from Hangzhou Chemer Chemical Co., Ltd. (China). MWCNTs (purity>95%) with an average diameter of 10-20 nm were purchased from Shenzhen nanotech port Co., Ltd. (China). All the electrodes were purchased from Tianjin Aida Co., Ltd (China). All the chemicals were of analytical grade and used as-received without any further treatment. Deionized water was used to prepare the aqueous solutions.

2.2 Preparation of $Pd_xNi_yFe_z$/MWCNTs trimetallic composite nanoparticles

Firstly, 4.1 mg PdO and proper amounts of $NiCl_2$ and $FeCl_3$ were dissolved in 4 mL [BMIM]OTF to prepare a solution, and it should be noted that the added amounts of $NiCl_2$ and $FeCl_3$ were determined based on the atomic ratio of Pd:Ni:Fe. That is to say, the amount of PdO was kept identical and the amounts of $NiCl_2$ and $FeCl_3$ were adjusted correspondingly. The samples, having the atomic ratios of Pd:Ni:Fe equivalent to 1:1:1,1:1.5:1,1:1:1.5,1:1:3 and 1:0:3, respectively, were denoted as sample a, b, c, d and e. Subsequently, 15 mg MWCNTs were added to the above solution, following 30 min ultrasonication. The resultant suspension solution was placed in a home-made autoclave, and then the well-sealed autoclave was transferred to a muffle furnace. The temperature of the muffle furnace was maintained at 200 ℃ for 3 hours to accomplish the pyrolysis process, which was carried out in an SRJX-8-13 muffle furnace equipped with a KSY 12-16 furnace temperature controller. After cooling down to the room temperature, the samples were filtered and dried in ambient condition to generate $Pd_xNi_yFe_z$/MWCNTs catalysts.

2.3 Fabrication of $Pd_xNi_yFe_z$/ MWCNTs modified electrode

A glassy carbon (GC) (geometric area of 0.07 cm^2) electrode was polished with 50 nm alumina nanopowder suspensions, and then served as a substrate for the working electrode. The working electrodes were fabricated by coating catalyst ink onto the well treated GC electrode. The catalyst ink was prepared by dispersing 1 mg catalyst in 1 mL Nafion ethanol solution (0.1 wt.%). And after ultrasonication for 30 min, about 10 μL ink was added on the surface of the GC electrode. Finally, the $Pd_xNi_yFe_z$/MWCNTs-coated GC electrode was fabricated after drying in air atmosphere.

2.4 Characterizations

XRD analysis of the catalysts was carried out on a Bruker D8 ADVANCE X-ray diffractometer equipped with a Cu Kα source (λ= 0.154 nm) at 40 kV and 30 mA. The 2θ angular region between 10 and 90° was explored at a scan rate of 1°/step. The particle morphology was observed by scanning electron microscopy (SEM, HITACHI, S-570) and transmission electron microscopy (TEM, HITACHI, H-7650). Energy Dispersive X-Ray Spectroscopy (EDX) spectrum analysis was carried out on a X-ray energy instrument (EDAX, PV-9900, USA). Electrochemical measurements were carried out on a CHI 660B electrochemical working station (Shanghai Chenhua Apparatus, China) connected to a personal computer.

A $Pd_xNi_yFe_z$/MWCNTs modified GC electrode, a platinum wire and a saturated calomel electrode (SCE) were used as the working electrode, counter electrode and reference electrode, respectively. Thus, all potentials in this paper were reported with respect to the SCE electrode. A solution of 1 M KOH containing 1 M C_2H_5OH was used to study EOR activity. All the experiments were carried out at room temperature.

3. RESULTS AND DISCUSSION

3.1 XRD Analysis

Figure 1 shows all the XRD patterns for the as-prepared samples. Evidently, the diffraction peak positioned at around 26° can only be indexed as the (002) facet of MWCNTs based on our previous works concerning MWCNTs [18]. To one's surprise, for all the samples, only the characteristic reflection peaks of the face centered cubic (fcc) crystalline Pd (JCPDS, Card No.01-087-0638) are displayed. Namely, the main reflection peaks at 2θ values of about 40, 47, 68 and 82°, respectively, correspond to the planes (111), (200), (220) and (311) of fcc crystalline Pd. This result is well consistent with the previous report [19]. After close inspection, the following conclusions could be achieved. First, no evident shifting of the diffraction peak position was observed when varying the atomic ratios, which effectively demonstrated that the prepared samples were composites rather than alloys [20]. Second, although the diffraction peak positions were not changed with the atomic ratios, the intensities of the diffraction peaks for all the samples changed significantly when the atomic ratios were varied. It seemed that sample **c** showed more sharper diffraction peaks as compared to other catalysts, which suggested that the crystallinity of $Pd_1Ni_1Fe_{1.5}$/MWCNTs is superior to other samples [21]. Third, no diffraction peaks of impurities were exhibited, indicative of the absence of impurities. It is well known that the contents of oxygen and water in the RTILs of [BMIM]OTF are very lower due to the unique properties of RTIL [22, 23], which probably may account for the absence of impurities in the resultant samples.
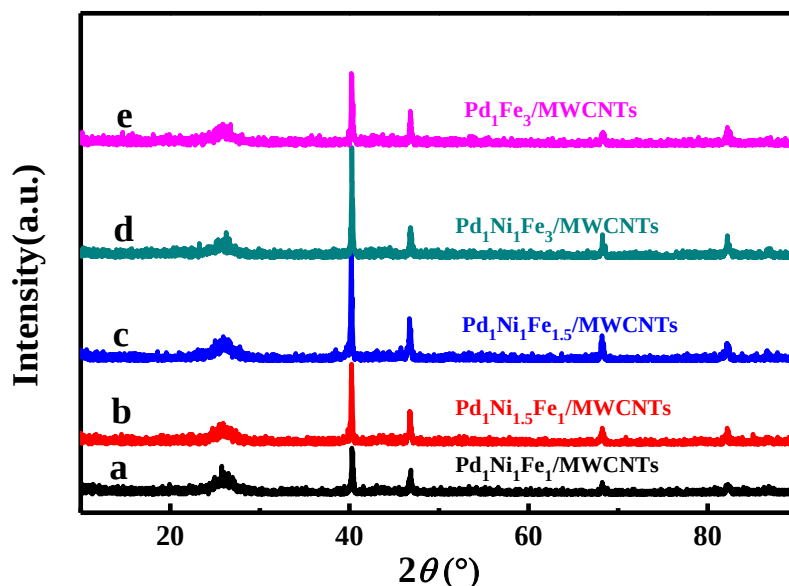
Figure 1. XRD patterns for the obtained samples of $Pd_xNi_yFe_z$/MWCNTs. Pattern **a, b, c, d** and **e** correspond to $Pd_1Ni_1Fe_1$, $Pd_1Ni_{1.5}Fe_1$, $Pd_1Ni_1Fe_{1.5}$, $Pd_1Ni_1Fe_3$ and Pd_1Fe_3-coated MWCNTs.
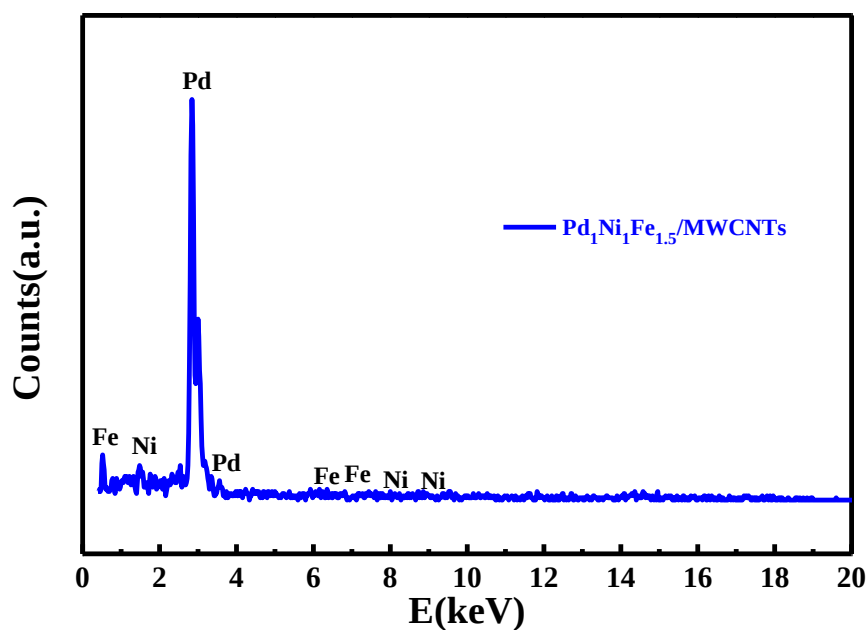
Figure 2. EDX spectrum for the typical catalyst of $Pd_1Ni_1Fe_{1.5}$/MWCNTs.

Figure 2 shows the typical EDX spectrum for the particles of $Pd_1Ni_1Fe_{1.5}$/MWCNTs catalyst, in which the peaks corresponding to the elements of Pd, Ni and Fe are displayed clearly. And no elements of O and Cl were found, which substantially indicated that all the starting materials of metal salts were reduced in above pyrolysis process. The atomic ratio of Pd:Ni:Fe was 97.78:1.96:0.26, which rather did not accord with the atomic ratio in the starting materials. Thus, the prepared composite particles should be noted as the nominal particles of $Pd_xNi_yFe_z$.

How does one comprehend the formation process of $Pd_xNi_yFe_z$ composite particles? It has been addressed that due to the self-oxidation process of carbon nanotubes some organic groups were formed on the surface of MWCNTs [24]. Thus, MWCNTs were probably utilized as reducing agents which could react with precursors to generate composite particles in above pyrolysis process. Meanwhile, the standard electrode potential of PdO ($E^{\Theta}_{Pd^{2+}/Pd}$=0.915V vs. NHE) is much higher than that of $NiCl_2$ ($E^{\Theta}_{Ni^{2+}/Ni}$=-0.257V vs. NHE) and $FeCl_3$ ($E^{\Theta}_{Fe^{3+}/Fe}$=0.771V vs. NHE) [25], therefore, the reaction velocity of the reaction between PdO and MWCNTs should be much faster than other two reactions (i.e., $NiCl_2$ with MWCNTs, and $FeCl_3$ with MWCNTs) under the same preparing conditions. That is to say, metallic Pd was formed first in above pyrolysis process, and then metallic Fe and Ni probably were produced at the outer surface of Pd particles, leading to the formation of nominal trimetallic particles of $Pd_xNi_yFe_z$.

3.2 Morphology characterization

Figure 3 shows the SEM morphologies of the five catalysts. Obviously, for all the samples, some irregular large particles were immobilized on the surface of MWCNTs after the pyrolysis process, which strongly demonstrated the presence of reactions between the precursors and MWCNTs in the RTILs system. The particles sizes for sample a, b, c, d and e were estimated be around 600, 228, 107, 226 and 642 nm, respectively. Thus, sample **c** displayed the smallest particle size among all the samples, which may provide larger surface area when the loadings of catalysts were identical. Also, it can be seen that the large particle of sample **e** consisted of many smaller particles, and some MWCNTs were wrapped into the resultant large particles. This result indicated that the aggregation of particles occurred in the case of sample **e**. Above observations effectively testified that the atomic ratio in the starting materials was a key factor that could significantly influence the morphology of the resultant samples. To the best of our knowledge, this is the first time to present the SEM images of $Pd_xNi_yFe_z$ particles though numerous works concerning Pd-based bimetallic composite or alloyed particles have been published so far.

The TEM microstructures of these five samples are illustrated in Figure 4. Evidently, some particles are observed to be coated on the MWCNTs, further indicating the formation of composite particles. The particle sizes of the sample a, b, c, d and e were evaluated to be 100, 357,114 and 392 nm based on the TEM images, respectively. Interestingly, no evident particles were observed in the TEM image. The fact, that the particle sizes seen by SEM were larger than those observed in the TEM measurements, strongly demonstrated that the large particles shown in Figure 3 were composed of many smaller particles. That is to say, agglomeration of smaller particles occurred in the pyrolysis process. It should be emphasized that pentagon and hexagon-shaped regular crystal particles were, respectively, formed in the case of sample c and d. Ordinarily, the properties of RTILs such as dielectric constant and diffusion coefficient were very distinguished from those of water. Thus, it is reasonable to believe that the formation of Pd-based pentagon or hexagon-shaped crystal particles was originated from the peculiar property of RTILs. This is the first time to report the pentagon and hexagon-shaped crystal particles of Pd-based composite, to our knowledge.
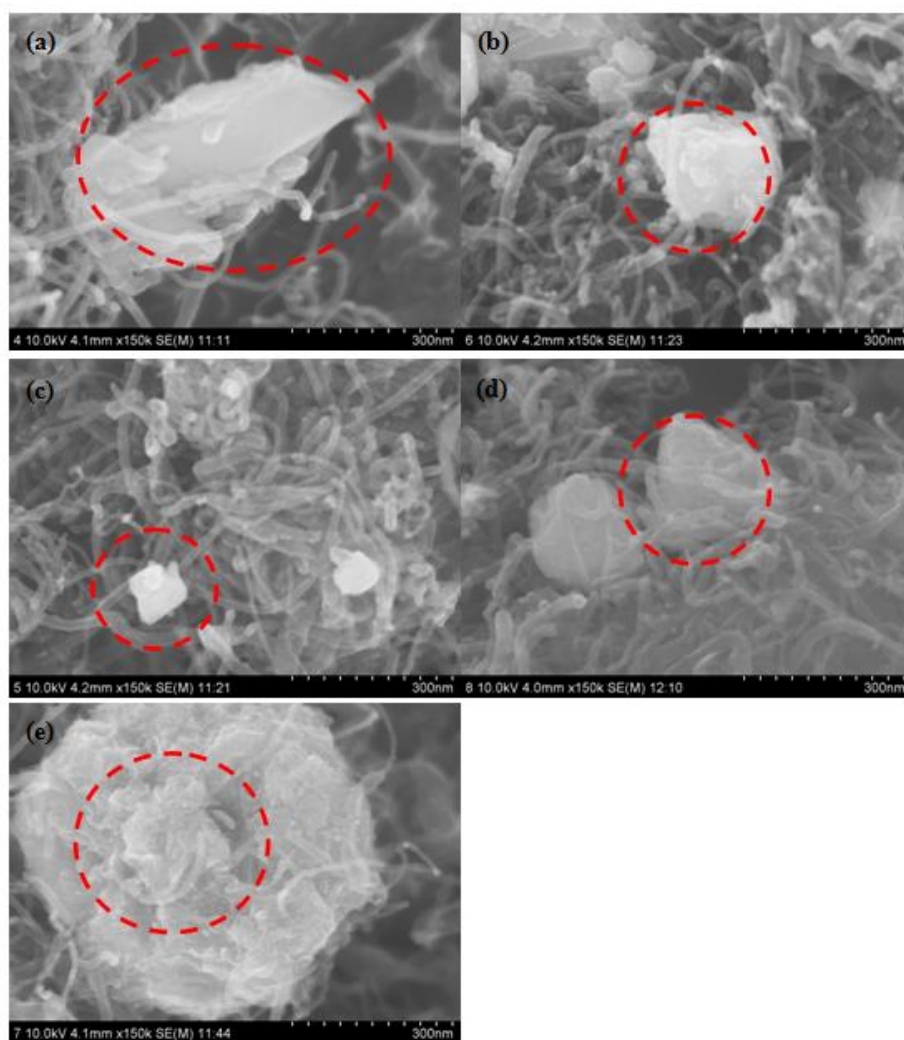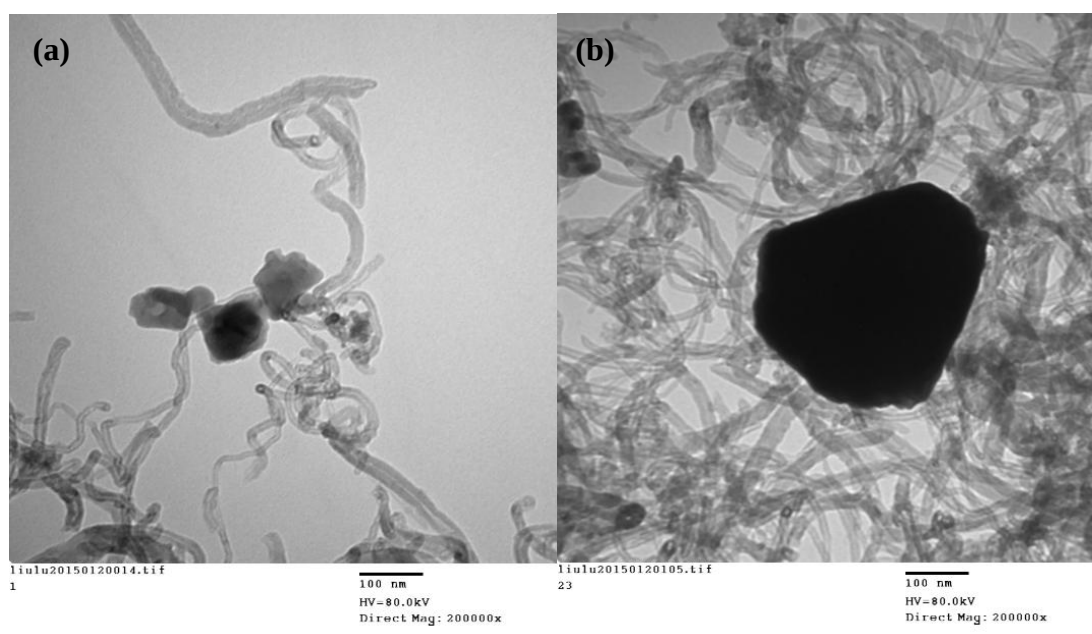
Figure 3. SEM images for the obtained samples of $Pd_xNi_yFe_z$/MWCNTs. Image **a, b, c, d** and **e** correspond to $Pd_1Ni_1Fe_1$, $Pd_1Ni_{1.5}Fe_1$, $Pd_1Ni_1Fe_{1.5}$, $Pd_1Ni_1Fe_3$ and Pd_1Fe_3-coated MWCNTs.
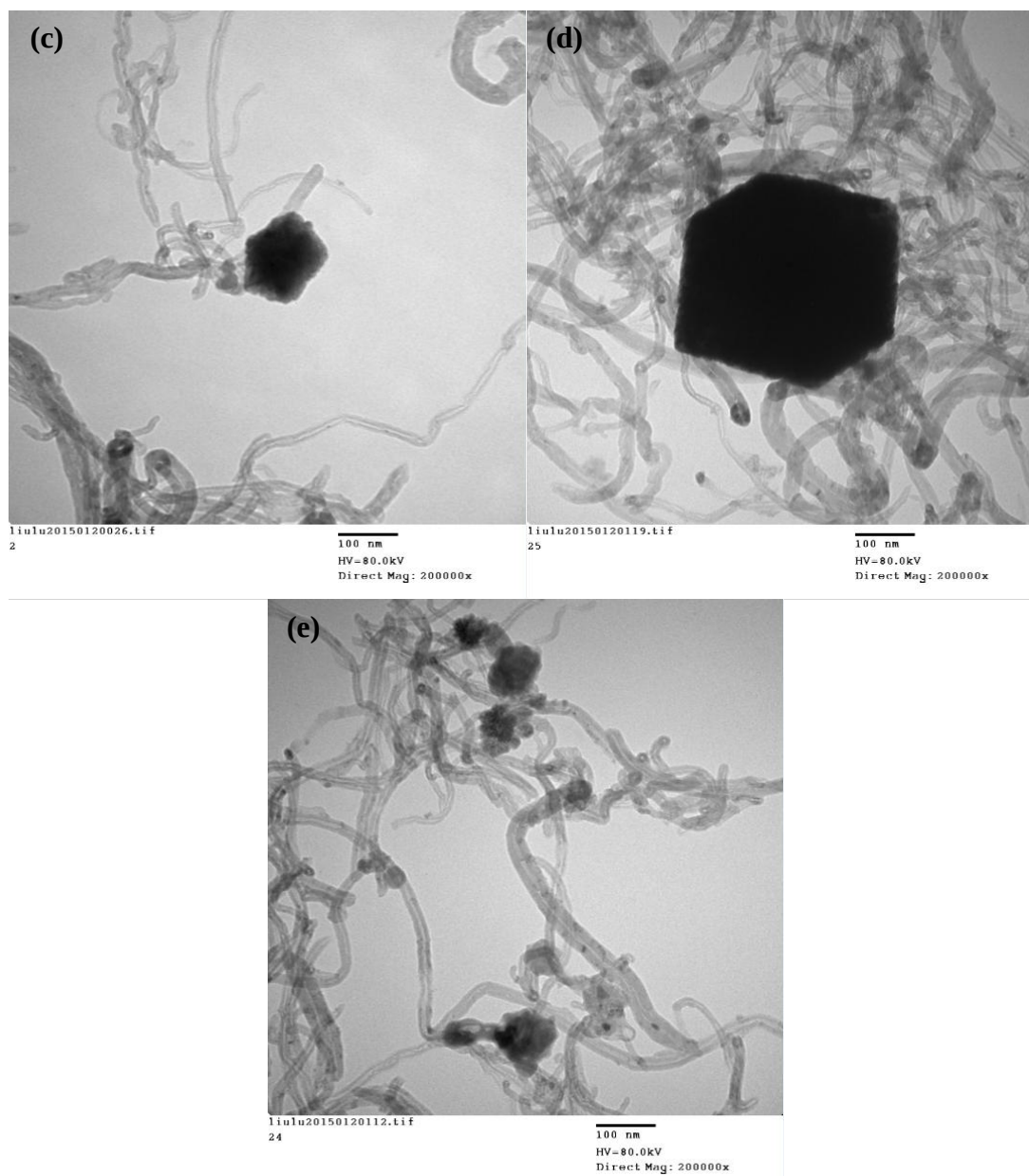
Figure 4. TEM images for the obtained samples of $Pd_xNi_yFe_z$/MWCNTs. Image **a, b, c, d** and **e** correspond to $Pd_1Ni_1Fe_1$, $Pd_1Ni_{1.5}Fe_1$, $Pd_1Ni_1Fe_{1.5}$, $Pd_1Ni_1Fe_3$ and Pd_1Fe_3-coated MWCNTs.

3.3. Electrochemical characterization

The cyclic voltammograms (CVs) of the $Pd_xNi_yFe_z$/MWCNTs catalysts in a solution of 1 M KOH containing 1M C_2H_5OH were given in Figure 5. For all the cases, two oxidation peaks (one at ~-0.28 V in the anodic sweep curve (peak **1**) and the other one at ~-0.42 V in the cathodic sweep (peak **2**)) were displayed clearly. The shape of CVs presented here is very similar as the reported one that was obtained on the Pd-coated GC electrode [26]. This strongly indicated that EOR could proceed on all the prepared catalysts. As shown by the blue line, for both peak **1** and peak **2**, the largest peak current for the EOR was exhibited on the catalyst of $Pd_1Ni_1Fe_{1.5}$/MWCNTs, which implied that $Pd_1Ni_1Fe_{1.5}$/MWCNTs possessed the best electro-catalytic ability towards EOR when compared to

other catalysts. The smallest particle size of $Pd_1Ni_1Fe_{1.5}$ probably may account for its excellent electrocatalytic activity as compared to other catalysts studied in this work. This result, at least, proved that the trimetallic composite particles containing Pd, Ni and Fe could be used as catalysts towards EOR and the atomic ratio of Pd, Ni and Fe played an important role in determining the final electrocatalytic ability of the resultant catalysts.
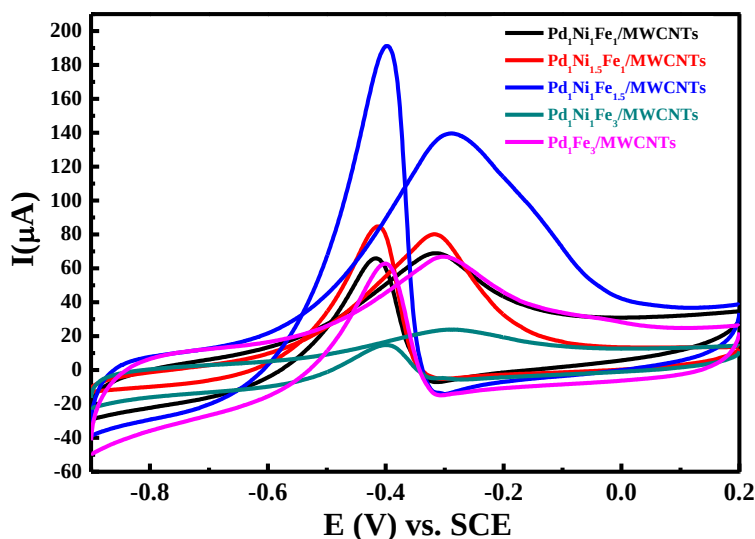
Figure 5. Cyclic voltammograms (CVs) obtained on the prepared $Pd_xNi_yFe_z$/MWCNTs-coated GC electrodes in 1M KOH+1M C_2H_5OH solution at the scan rate of 50 mVs^{-1}. The black, red, blue, green and pink curves were recorded on the $Pd_1Ni_1Fe_1$, $Pd_1Ni_{1.5}Fe_1$, $Pd_1Ni_1Fe_{1.5}$, $Pd_1Ni_1Fe_3$ and Pd_1Fe_3/MWCNTs catalysts.
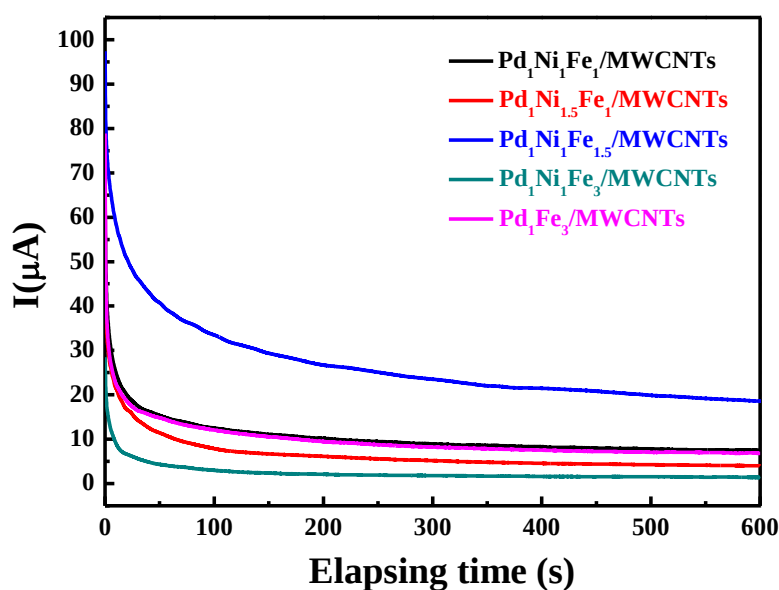
Figure 6. Chronoamperometry curves of the as-prepared samples-coated GC electrode in 1M KOH +1M C_2H_5OH at -0.24V. The black, red, blue, green and pink curves were recorded on the $Pd_1Ni_1Fe_1$, $Pd_1Ni_{1.5}Fe_1$, $Pd_1Ni_1Fe_{1.5}$, $Pd_1Ni_1Fe_3$ and Pd_1Fe_3/MWCNTs catalysts, respectively.

To research the electrochemical stability of all the prepared catalysts toward EOR, chronoamperometric curves of 1 M KOH solution containing 1M C_2H_5OH at the $Pd_xNi_yFe_z$/MWCNTs-modified GC electrodes at -0.24 V were recorded as shown in Figure 6 [27]. For all the curves, a sharp decrease of the current in the initial stage was followed by a relatively stable current in the left testing period. Apparently, the catalyst of $Pd_1Ni_1Fe_{1.5}$ delivered the highest current in the whole testing period. For example, the currents at the catalysts of **a**, **b**, **c**, **d** and **e** are about 7.4, 3.5, 18.5, 1.1 and 7.0 μA at 600 s, respectively. This result also effectively confirmed that the catalyst of $Pd_1Ni_1Fe_{1.5}$/MWCNTs showed the best stability among all the prepared samples when used as a catalyst toward EOR, which was perhaps due to its smaller particle size or some unknown synergetic effects.

Why did the $Pd_xNi_yFe_z$ catalysts with various molar ratios show such different electrocatalytic activity for EOR? To offer the possible explanations, the curves of open circuit potentials against time for these five catalysts-coated GC electrodes in 1 M KOH were plotted as shown in Figure 7.
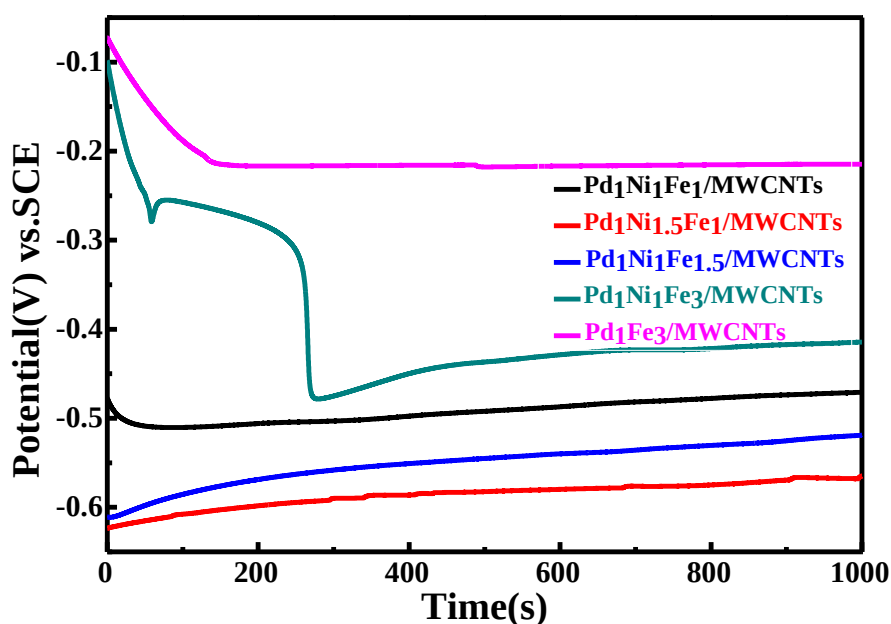
Figure 7. Open circuit potentials of various catalyst modified GC electrodes in 1M KOH solution. The black, red, blue, green and pink curves were recorded on the $Pd_1Ni_1Fe_1$, $Pd_1Ni_{1.5}Fe_1$, $Pd_1Ni_1Fe_{1.5}$, $Pd_1Ni_1Fe_3$ and Pd_1Fe_3/MWCNTs catalysts, respectively.

Figure 7 displays the curves of open circuit potential (OCP) as a function of time. A sharp decrease of OCP value is observed for the catalysts of a, d and e within the initial period time of around 100 s. In contrast, an evident increment of OCP value is seen for the catalysts of b and c in the initial testing time of 150 s. For all the cases, the value of OCP reached a stable status after a certain period. The significantly different OCP curves exhibited by the catalysts, explicitly, were originated from the diverse interactions between the catalysts and electrolyte of 1M KOH, since the OCP value of an electrode was mainly decided by the its nature. Meanwhile, the OCP values for the catalysts were

different from each other, that is to say, the atomic ratio of Pd, Ni and Fe in the resulting catalysts greatly influenced its OCP value. For instance, at the working time of 1000 s, the values of COP for the catalysts of a, b, c, d and e were about -0.47, -0.57, -0.52, -0.41 and -0.21 V, respectively. Except for catalyst of $Pd_1Ni_{15}Fe_1$, the lowest value of OCP is presented by the catalyst of $Pd_1Ni_1Fe_{1.5}$. This result suggested that the electrons can be released from the catalyst of $Pd_1Ni_1Fe_{1.5}$ easier than the other catalysts according to the Nernst Equation [28], thus, probably prior to the electro-oxidation of ethanol the catalyst of $Pd_1Ni_1Fe_{1.5}$ was electro-oxidized to a transition state. And this newly developed transition state is beneficial to the adsorption as well as the electrooxidation of ethanol, as a result, the largest peak current of EOR was exhibited by the catalyst of $Pd_1Ni_1Fe_{1.5}$.

4. CONCLUSION

For the first time, a series of $Pd_xNi_yFe_z$ catalysts were prepared by a pyrolysis approach using RTILs of 1-n-Butyl-3-methylimidazolium triflate ([BMIM]OTF) as the solvent in the presence of MWCNTs. The results demonstrated that due to the smaller particle size and relatively lower value of OCP, the $Pd_1Ni_1Fe_{1.5}$/MWCNTs catalyst exhibited the best electrocatalysis toward EOR among all the prepared catalysts. Successful preparation of a trimetallic nanopaticle of $Pd_xNi_yFe_z$ by a pyrolysis process and describing its electrocatalytic performance towards EOR are the main contributions of this preliminary work. This work is believed to be very helpful for developing novel catalysts towards small organic molecules oxidation reaction, as well as extending the applications of RTILs.

References

1. W. Du, G. Yang, E. Wong, N. Deskins, A. Frenkel, D. Su and X. Teng, *J. Am. Chem. Soc.*, 136 (2014) 10862.
2. D. Kwak, Y. Lee, S. Han, E. Hwang, H. Park, M. Kim and K. Park, *J. Power Sources*, 275 (2015) 557.
3. A. Dutta and J. Ouyang, *ACS Catal.*, 5 (2015) 1371.
4. V. Comignani, J. Sieben, M. Brigante and M. Duarte, *J. Power Sources*, 278 (2015) 119.
5. K. Ding, Y. Wang, H. Yang, C. Zheng, Y. Cao, H. Wei, Y. Wang and Z. Guo, *Electrochim. Acta*, 100 (2013) 147.
6. Y. Zhou and D. Zhang, *J. Power Sources*, 278 (2015) 396.
7. J. Ryu, J. Choi, D. Lim, H. Seo, S. Lee, Y. Sohn, J. Park, J. Jang, H. Kim, S. Hong,P. Ki and S. Yoo, *Appl. Catal. B: Environ.*, 174-175 (2015) 526.
8. M. Jeon and P. McGinn, *J. Power Sources*, 194 (2009) 737.
9. J. Jacob, P. Corradini, E. Antolini,N. Santos and J. Perez, *Appl. Catal. B: Environ.*, 165 (2015)176.
10. D. Chu, Z. Li, X. Yuan, J. Li, X. Wei and Y. Wan, *Electrochim. Acta*,78 (2012) 644.
11. P. Corradini,E. Antolini and J. Perez, *J. Power Sources*, 275 (2015) 377.

12. Y. Feng, Z. Liu, Y. Xu, P. Wang, W. Wang and D. Kong, *J. Power Sources*, 232 (2013) 99.
13. A. Dutta, S. Mahapatra and J. Datta, *Int. J. Hydrogen Energy*, 36 (2011) 14898.
14. Y. Wang, K. Jiang and W. Cai, *Electrochim. Acta*, 162 (2015) 100.
15. J. Li, Z. Zhu, S. Yang, Z. Zhang, W. Wu and H. Jiang, *J. Org. Chem.*, 80 (2015) 3870.
16. A. Jones, H. Kronenwetter and R. Manchanayakage, *Electrochem. Commun.*, 25 (2012) 8.
17. K. Ding and G. Yang, *Electrochim. Acta*, 55 (2010) 2319.
18. K. Ding and M. Cao, *Russ. J. Electrochem.*, 44 (2008) 977.
19. H. Boehm ,*Adv. Catal.*, 16 (1966) 179.
20. W. He, J. Liu, Y. Qiao, Z. Zou, X. Zhang, D. Akins and H. Yang, *J. Power Sources*, 195 (2010) 1046.
21. K. Ding, H. Yang, Y. Cao, C. Zheng, S. Rapole and Z. Guo, *Mater. Chem. Phys.*, 142 (2013) 403.
22. K. Ding, L. Liu, Y. Cao, X. Yan, H. Wei and Z. Guo, *Int. J. Hydrogen Energy*, 39 (2014) 7326.
23. K. Ding, J. Chin. *Chem. Soc.*, 54 (2007) 1179.
24. K. Ding, Y. Zhao, L. Liu, Y. Cao, Q. Wang, H. Gu, X. Yan and Z. Guo, *Int. J. Hydrogen Energy*, 39 (2014) 17622.
25. A. Bard, L. Faulkner, *Electrochemical methods fundamentals and applications*, 2nd Edition. Published By John Wiley& Sons, Inc. 2001.
26. K. Ding, G. Yang, S. Wei, P. Mavinakuli and Z. Guo, *Ind. Eng. Chem. Res.*, 49 (2010) 11415.
27. E. Monyoncho, S. Ntais, F. Soares, T. Woo and E. Baranova, *J. Power Sources*, 287 (2015) 139.
28. P. Ju, Y. Zuo, Y. Tang and X. Zhao, *Corros. Sci.*, 66 (2013) 330.